SPARC_LAB activities and achievements

M.P. Anania, S. Arjmand (Dott.), M. Behtouei, M. Bellaveglia, A. Biagioni,
E. Chiadroni (Ass.), A. Cianchi (Ass.), G. Costa, A. Del Dotto, M. Del Giorno (Tecn.),
F. Dipace (Dott.), M. Ferrario (Resp.), M. Galletti (Ass.), L. Giannessi, A. Giribono,
P. Iovine (Dott.), V. Lollo (Tecn.), A. Mostacci (Ass.), G. Di Pirro, R. Pompili, S. Romeo,
V. Shpakov, C. Vaccarezza, F. Villa, A. Zigler (Ass.)

1 Introduction

The program of the SPARC_LAB [1] for 2021 has actually started from the experimental findings of the previous year related to the first plasma accelerated electron beams [2]. These results have been firstly improved at the beginning of the year thanks to a modification of the plasma module. Then the experimental program regarded the use of the plasma accelerated beams to drive a Free-Electron Laser (FEL) operating in the Self Amplified Spontaneous Emission (SASE). The successful operation of the FEL and the main achievements are described in the following.

2 Improvements on the plasma accelerator module

In 2020 the first demonstration of plasma acceleration was obtained by sending two consecutive bunches, a 200 pC driver followed by a 20 pC witness, into the plasma generated in a 3 cm-long capillary. Accelerating fields as large as 200 MV/m were obtained from the driver and transferred to the witness, gaining up to 6 MeV into the plasma. However, the observation of the first plasma accelerated beams highlighted rather large energy fluctuations. Further studies identified two main causes of such energy instabilities related to (i) the plasma formation process and (ii) the RF timing-jitter affecting the driver-witness separation. While a solution to the second one is still under study and would probably require a replacement of the current PFN modulators with new ones employing solid-state technology, we identified that the instabilities on the plasma were related to a non-proper discharge process happening in the capillary. The plasma is indeed generated started from hydrogen gas by an high-voltage (HV) discharge current applied to the two electrodes at the capillary ends. We found that such a discharge was not always flowing through the capillary (between the two electrodes) but was often deviating from one electrode making its ground on the fast electro-valve located nearby. We solved such an issue by slightly moving away the electro-valve from the two electrodes and by electrically insulating it from the rest of the apparatus. This fix produced stable HV discharge through the capillary for all the following experimental runs. A second improvement for the plasma discharge stability consisted in the use of an external laser [3]. The stability and repeatability of the plasma formation is indeed enhanced by pre-ionizing the gas with a Nd:YAG laser focused at the capillary entrance. This reduced the discharge timing-jitter from tens to few nanoseconds and, in turn, the plasma density fluctuations from 12% to 6%.

3 Plasma Acceleration

The plasma accelerator module consists of a 3D-printed capillary with length $L_p = 3$ cm and 2 mm diameter. The capillary is filled with Hydrogen gas through two symmetric inlets. The plasma

is generated by ionizing the gas with a high-voltage discharge providing 5 kV pulses with 120 A current and ≈ 1 μs duration. Two triplets of movable permanent-magnet quadrupoles (PMQ) are installed upstream and downstream the capillary to focus the beam into the plasma and extract from it after acceleration.
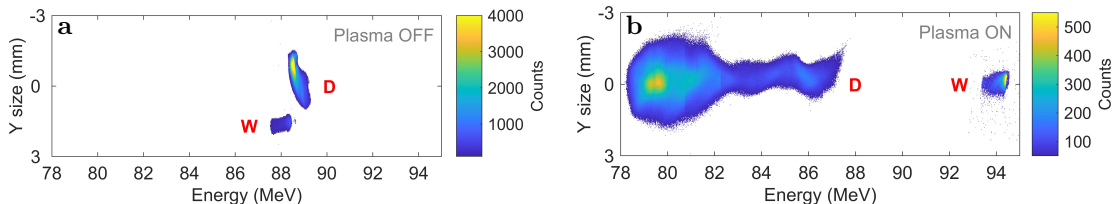
Figure 1: **Witness acceleration in plasma.** Snapshots of the driver (D) and witness (W) spectrum with plasma turned off (a) and on (b). In (a) the RF-Deflector is turned on to vertically separate the two bunches. In (b) the decelerated driver energy spectrum is obtained by merging the images obtained with different currents of the spectrometer.

The experiment is performed by using a driver and witness bunches separated by $\Delta t = 1.21 \pm 0.02$ ps. These are focused at the plasma entrance with a triplet of permanent-magnet quadrupoles (PMQs) down to $\sigma_{r,d} = 20 \pm 1$ μm and $\sigma_{r,w} = 14 \pm 1$ μm, respectively. The driver charge is $Q_d = 200 \pm 5$ pC with duration $\sigma_{t,d} = 215 \pm 5$ fs. For the witness the charge is $Q_w = 20 \pm 2$ pC and $\sigma_{t,w} = 30 \pm 3$ fs the duration. With the plasma turned off, the driver energy is $E_d = 88.5 \pm 0.1$ MeV with energy spread $\sigma_{E,d} = 0.23 \pm 0.01$ MeV while for the witness $E_w = 88.1 \pm 0.1$ MeV and $\sigma_{E,w} = 0.31 \pm 0.02$ MeV. Figure 1(a) shows the longitudinal phase-space (LPS) of the driver and witness bunches prior the plasma acceleration module. By turning on the plasma and setting its density to $n_e \approx 1.6 \times 10^{15}$ cm^{-3}, we obtain the spectrum showed in Fig. 1(b). The plot shows both the accelerated witness and the decelerated driver. The latter one has been reconstructed by merging the images obtained with different currents of the magnetic spectrometer.

Considering 500 consecutive shots of the accelerated witness, its energy and energy spread distributions are reported in Fig. 2. The resulting average energy is $E_w = 93.9 \pm 0.3$ MeV, corresponding to ≈ 200 MV/m accelerating gradient. The achieved 0.3 MeV energy-jitter is mainly due to fluctuations of the driver-witness distance and plasma density. The energy spread of the accelerated witness is preserved, $\sigma_{E,w} = 0.31 \pm 0.08$ MeV

4 SASE Free-electron lasing with the plasma accelerated witness

The experimental setup of the FEL experiment is showed in Fig. 3. The FEL beamline consists of six undulators, each one 2.15 m long with 77 periods with period $\lambda_u = 2.8$ cm. A quadrupole is installed between two consecutive undulators to transport the beam. The gap of each undulator can be tuned to adjust the undulator parameter in the range $K_u \approx 0.4 \div 3$. Downstream each undulator, an in-vacuum metallic mirror can be inserted to send the FEL radiation to a calibrated photo-diode. At the exit of the last undulator the radiation spectrum is also measured with an imaging spectrometer equipped with a diffraction grating and a cooled intensified camera (iCCD).

Downstream the capillary, the beam is extracted by means of the second PMQ triplet and matched into the FEL beamline. Passing through the undulators, the beam produces FEL radiation with spectrum peaked at a resonance wavelength $\lambda_r = \lambda_u \left(1 + K_u^2/2\right)/2\gamma^2 \approx 830$ nm, where γ is the relativistic Lorentz factor and $K_u \approx 1.4$. A proof of the light amplification along the undulators is provided by measuring the growth of the pulse energy after each undulator with the photo-diodes.
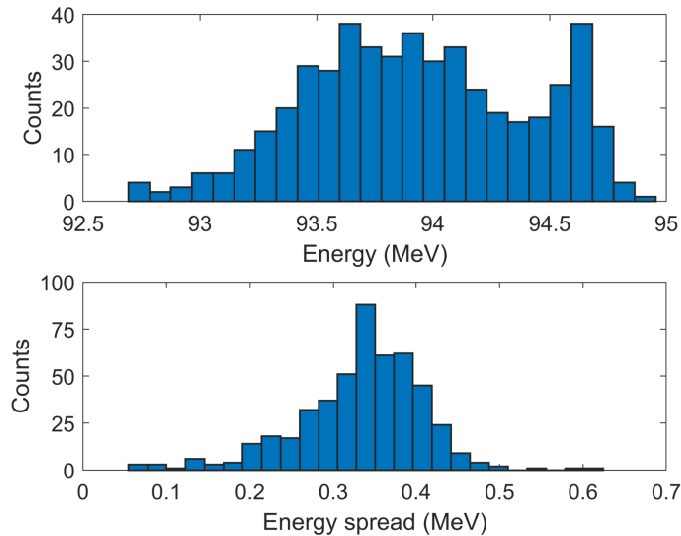
Figure 2: **Data collected for the witness bunch**. Energy (top) and spread (bottom) distributions of 500 consecutive shots of the accelerated witness.

Figure 4 shows the resulting energies (E_{pd}) measured by the six photo-diodes as a function of the longitudinal coordinate (z) where the light is extracted from the undulators beamline. For each photo-diode were acquired 200 consecutive shots. The values reported correspond to the average energy measured considering only the 10% most intense pulses. An average background signal resulting from the energy-depleted driver was separately measured by turning off the witness and then subtracted. The red line shows the numerical fit $(R^2 \approx 0.9997)$ computed on the measured energy according to the exponential law $E_{pd} = a \cdot \exp{(z/L_g)}$, where $L_g = 1.1 \pm 0.1$ m is the resulting gain length.

Such a proof-of-principle experiment demonstrated the first lasing of a FEL driven by a PWFA. The results indicate that the high-quality of the plasma accelerated beam (with low energy spread and emittance), accompanied by the high stability and reproducibility of the acceleration process, allowed to transport the beam along a segmented undulators beamline and amplify FEL light in the near-infrared range. The achieved FEL performances well match the theoretical expectations thanks to the precise knowledge of the beam phase-space, completely characterized from injection and propagation in the plasma up to the capture at its exit. It represents an important contribution in view of EuPRAXIA, a future PWFA-based user-facility able to drive a X-rays FEL.

5   Seeded Free-electron lasing with the plasma accelerated witness

On the way of the encouraging results achieved with FEL, we were able also to test the FEL operation in the seeded regime, i.e. when the FEL emission is triggered by an external laser. In a SASE FEL, indeed, the amplification process starts from an initial shot-noise in the electron beam current. Therefore the stability and reproducibility of the emitted radiation may be not adequate to be adopted in user applications. For this reason many FELs operate nowadays in the seeded regime. Such a further step represents the first proof-of-principle experiment demonstrating stable generation of intense amplified radiation from a FEL driven by a centimeter-scale plasma accelerator. By using an external seed laser, FEL radiation is obtained at $\lambda_r \approx 827$ nm and improved in terms of output energy (≈ 1.1 μJ) and stability ($\approx 90\%$). Such enhancements are
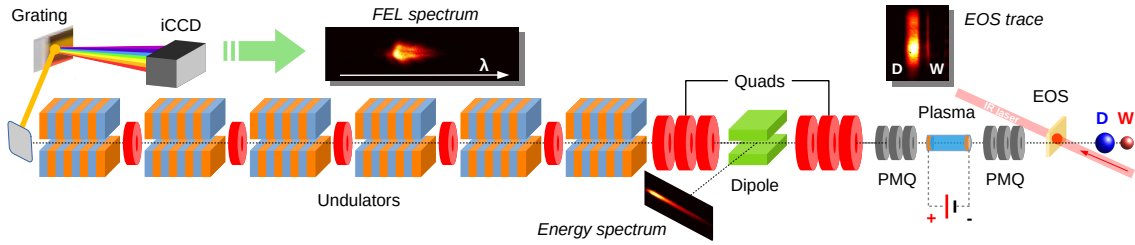
Figure 3: **Experimental setup.** The driver (D) and witness (W) electron bunches are produced by the photo-injector and their temporal separation is continuously monitored with a non-intercepting EOS diagnostics. The bunches are focused by a triplet of PMQs in a 3 cm-long capillary containing the plasma produced by ionizing Hydrogen gas with a high-voltage discharge. The accelerated witness is extracted by second triplet of PMQs and transported by using six electromagnetic quadrupoles. A dipole spectrometer is used to measure its energy with a scintillator screen installed on a 14° beamline. The FEL beamline consists of six planar undulators with tunable gaps and five quadrupoles in between to transport the beam. The emitted FEL radiation is collected by an in-vacuum metallic mirror and measured with an imaging spectrometer equipped with a diffraction grating and a cooled intensified camera (iCCD).

clearly evident by comparing these numbers to the ones obtained in SASE regime, with $\approx 27\%$ stability and output energy below 30 nJ. A magnetic chicane is used to horizontally displace the beam prior to the undulators and allow the injection of the seed laser on the same path. The seed laser (centered at $\lambda_L = 797 \pm 3$ nm with 7 ± 1 nm bandwidth) has ≈ 20 nJ energy and ≈ 250 fs rms duration.

Figure 5 shows 100 consecutive shots acquired in SASE (left) and seeded (right) configuration (seed laser turned off or on, respectively). A clear enhancement of the radiation reproducibility is noticeable when using the seed laser, resulting in a stability of $89\% \pm 3\%$, that in SASE is only $27\% \pm 5\%$. The obtained results indicate that the use of an external laser allows to seed the emission process and stabilize its amplification along six consecutive undulators. This strongly suppressed the fluctuations observed in previous experiments operating in the SASE regime.

References

1. M. Ferrario *et al*, Nuclear Instruments and Methods B 309, 183 (2013)

2. R. Pompili *et al*, Nature Physics , 1 (2021)

3. Biagioni A. *et al*, Plasma Physics and Controlled Fusion 63.11 (2021), 115013.
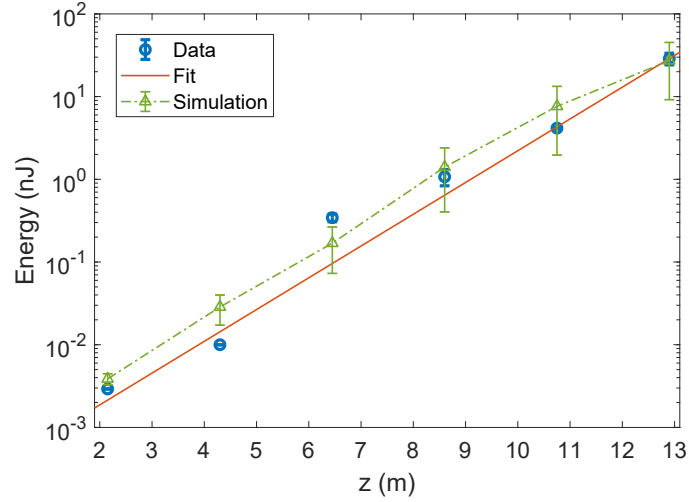
Figure 4: **Exponential growth of the amplified light.** Energy gain of the FEL radiation along the six undulators measured with the photo-diodes (blue circles). The (solid) red line shows the computed exponential fit over the experimental data. The resulting FEL simulation (green triangles) is also reported. The error bars are computed as the standard deviation of the signal amplitudes measured at each point.
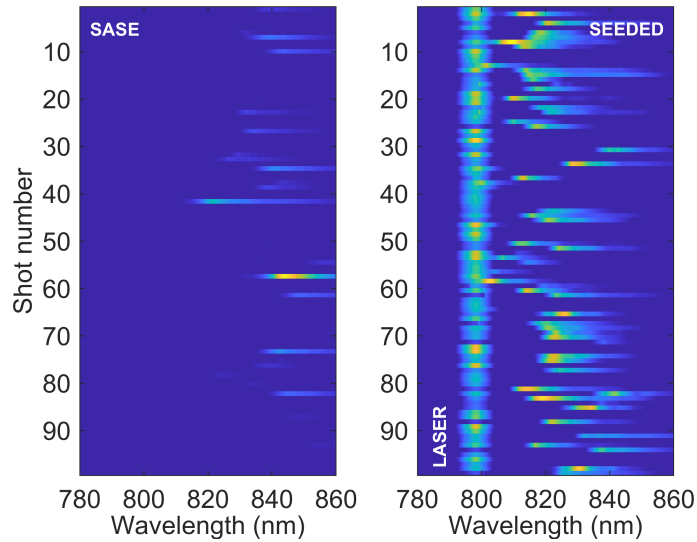
Figure 5: **Spectral analysis.** Comparison between 100 shots acquired in SASE and seeded FEL configurations with the seed laser turned off and on, respectively.